Chapter 2

Direct Dynamics Simulations of the Copper-Water Interface: Successes and Problems

Sean Walbran[1] and J. W. Halley[2]

[1]Forschungszentrum Jülich GmbH, Institut für Werkstoffe und Verfahren der Energietechnik (IVW–3), D–52425 Jülich, Germany
[2]School of Physics and Astronomy, University of Minnesota, Minneapolis, MN 55455

We report on direct dynamics studies of the electrode/electrolyte interface, in which the electronic structure of the electrode is calculated at each time step of a molecular dynamics simulation. Results for a model of the copper/water interface, in which copper pseudopotential centers are described with 4s electrons, are presented for two crystal faces. We discuss of our attempts to model the 3d electrons on the electrode using a number of new approaches, and describe the computational challenges for such a system. Finally, we describe recent work applying direct dynamics techniques to the aluminum/water interface.

Introduction

Processes and reactions at the electrode/electrolyte interface are fundamental to such technologies as batteries, fuel cells, photochemical cells, and chemical etching. They are at the root of electrochemistry, and play a large role in corrosion, stress corrosion cracking, toxic chemical abatement, and weathering processes important to industry and geoscience. The interplay among the solid electrode, liquid solvent, and ions of the electrolyte presents a significant challenge to traditional theoretical modeling, involving physics on a wide range of length and time scales. We have used direct dynamics simulations to study the electrode/ electrolyte interface, including the electronic structure of the electrode in a molecular dynamics simulation of the aqueous electrolyte. Here, we review our calculations(1) of the copper/water interface and its capacitance, discuss some attempts to extend the simulations to include the d electrons on copper, and report on recent results with an aluminum electrode.

In Solid-Liquid Interface Theory; Halley, J. Woods;
ACS Symposium Series; American Chemical Society: Washington, DC, 2001.

The Copper–Water Interface

The electrostatic potential drop across the electrode–electrolyte interface as a function of charge on the electrode is a fundamental property of the interface. It is known that the measured capacitance of metal/water interfaces includes contributions from the electrons of the metal electrode (2– *9*) , from the water near the surface ('Stern layer' contributions), and from the ions of the electrolyte. These contributions are not neatly separable, though they have sometimes been modeled as three capacitors in series. Calculations carried out in which the electronic and 'Stern layer' contributions are modeled together using a direct dynamics model for the interface(*10*) are described here. We model the ionic contributions using the traditional Gouy Chapman theory (*11*) but employing a method for determining the boundary condition for the continuum Gouy Chapman theory from the microscopic direct dynamics model. The results give a relatively parameter free representation of the electrostatic response.

As discussed in references 2– 9 and elsewhere, the response of the electrons of the metal to changes in the electrostatic potential of the metal relative to the electrolyte results in a significant contribution to the differential capacitance. It is also well known that the dielectric properties of the water near the metal–electrolyte interface contribute to the capacitance, as first recognized by Stern (*13*) . Both the electronic and 'Stern Layer' effects are treated together without artificial spatial separation in a first principles model (*10*) in which wave functions are recalculated together with the corresponding forces on the water molecules in the model at each step of a molecular dynamics simulation. The model used for the calculations described here is identical to that described in reference 10 except that an improved central potential model (*14*) has been used to model the water. We also modified the code to model the 111 as well as the 100 surfaces of copper. The model has the virtues of the one in reference 10 but also its limitations. In particular, only the s–like electrons of the metal are treated explicitly.

We studied the charge on the electrode as a function of the potential drop across the interface. Because we found that equilibration of the water in response to a change in the field took a long time (of order 50ps) it was found expedient to run a classical simulation (*14*) at each new field before initiating the direct dynamics equilibration at each field. Explicitly the simulation sample consisted, for the 100 surface, of 245 water molecules and 180 copper atoms periodically continued, in a cell of dimensions 80 au x 29 au x 29 au as in reference 9. As in that paper, for the 100 surface, the electronic wavefunctions were calculated in a 'small cell' of dimensions 40 au x 29 au x 29 au . For the 111 surface the water sample contained 216 water molecules, the unit cell had the dimensions 61.4 au x 33.6 au x 33.6 au (32.5 Å x 17.8 Å x 17.8Å), and the 'small cell' had dimensions 30.7 au x 33.6 au x 33.6 au . The time step used for integrating the motion was 0.5 fs. The sample was allowed to relax for approximately 80,000 time steps in the classical simulation, followed by 2,000 time steps of equilibration in the quantum mechanical simulation with the electrons frozen in place. Subsequently the system was run with full coupling between the electrons and all atomic centers for a further 3,000 time steps, with

statistical measurements made during the final 1,000 time steps. The sample was periodically repeated an infinite number of times in all three dimensions as described in reference 10 .

Though we can simulate the Stern and electronic contributions quite realistically with this model, a realistic simulation of the double layer region, including the ions of the electrolyte explicitly, remains beyond our simulation capacity at present if we wish to include a microscopic description of the solvent and electronic structure of the electrode in the simulation. On the other hand, because the length scale variations of the potentials in the double layer region are also larger, at low (~.001 – .01 M) ionic strengths, by about an order of magnitude, the mean field representation given by the classical Gouy–Chapman theory (*11*) is rather good in this region. To determine the capacitance of the entire system, we have coupled this theory in a self–consistent manner to the model for the region near the electrode described above.

One approach is to simply add the Gouy–Chapman capacitance in series with the capacitance of the Stern layer. This approach implicitly and unrealistically postulates a sharp interface between the Stern layer and the region in which the electrolyte can be treated by the Gouy–Chapman model. If such a sharp interface existed, then the boundary condition on the macroscopic electric field in the Gouy Chapman theory would be simply 4π times the charge σ applied to the electrode, leading to the usual series expression for the lumped capacitances. However, when the interface is not sharp, the boundary condition for the Gouy Chapman model can be estimated from the molecular dynamics simulation by calculating the macroscopic electric field at the plane $z = zc$ at which the model begins to represent the system by the Gouy–Chapman model. (This can be shown to be equivalent in the linear response regime to taking account of the nonlocal and/or inhomogeneous character of the dielectric response of the solvent.) The appropriate value of z_c is not known a priori.

Because the $E(z_c)$ so determined is not necessarily equal to $4\pi\sigma/\varepsilon_{bulk}$ where ε_{bulk} is the bulk dielectric constant of the solvent, then we cannot simultaneously 1) use $E(z_c)$ as a boundary condition, 2) retain charge neutrality of the interface, and 3) use the Gouy Chapman theory in its usual form with a constant value of ε for the solvent. A simple and physically reasonable path out of this situation is to adopt an extension of the Gouy Chapman model in which ffl varies smoothly with z from the simulation determined value $\varepsilon(z_c) = 4\pi\sigma/E(z_c)$ to the bulk value far from the electrode:

$$\varepsilon(z) = \varepsilon(z_c) + \left(\varepsilon_{bulk} - \varepsilon(z_c)\right)\left(1 - e^{\frac{-(z-z_c)}{z_o}}\right)$$

We found that the net capacitance which we calculated from the resulting model depended only weakly on the decay length, which was taken to be z_o = 5Å. (Taking ε

$z_o = 5 \pm 2$Å results in potential variances of $< 0.02V$ in capacitance plots such as those shown below.) With this form for $\varepsilon(z)$ we numerically solved the Poisson–Boltzmann equation for $z > z_c$, yielding the net potential drop from inside the electrode to the bulk of the solution as

$$\phi = \left(\phi_{MD}(z \to -\infty) - \phi_{MD}(z = z_c)\right) + \left(\phi_{GC}(z = z_c) - \phi_{GC}(z \to \infty)\right)$$

where $\phi_{MD}(z)$ is the electrostatic potential obtained from the simulation described in the last section. In practice, $z \to \infty$ is replaced by a point inside the model metal slab where the macroscopic field is essentially zero.

To obtain this $E(z_c)$, we calculated smoothed values of the macroscopic electric field E as found from the simulations at various planes z as a function of the electrode charge σ. The smoothing was accomplished by averaging the calculated fields over the xy plane and around each z value with a Gaussian weight of width 5 Å for the 111 surface and 7 Å for the 100 surface; this removes irrelevant fluctuations due to detailed molecular structure and corresponds to the standard definition of the macroscopic electric field (*17*). (The appropriate width of the Gaussian is not defined a priori and was chosen to be as small as possible to retain information about the change in field with distance from the electrode while minimizing noise; we were able to use a smaller width for the 111 surface in part because the simulation's cross–sectional area gave more water molecules per unit distance and hence less noise in the raw simulation data.)

An interesting feature of these results is that the macroscopic field can be lower near the interface than it is deep in the solvent. This is qualitatively different from results obtained from classical models (*15*), in which the fields near the interface are almost always higher than they are in bulk. The lower fields near the surface are due to the screening of the fields by the electrons of the metal, giving a smooth rise of the field from the bulk metal to the bulk solvent. We illustrate this effect explicitly in Figure 1.

Using the calculated macroscopic fields as boundary conditions, we determined the total electrostatic response of the interface with results shown for the two faces in Figures 2, 3, and 4.

Comparison with Experiment

The only undetermined parameter in this model for the structure of the interface is z_c, the point at which the continuum and simulation models are matched. In Figure 2 we show the comparison with experimental data from reference 17 for the 100

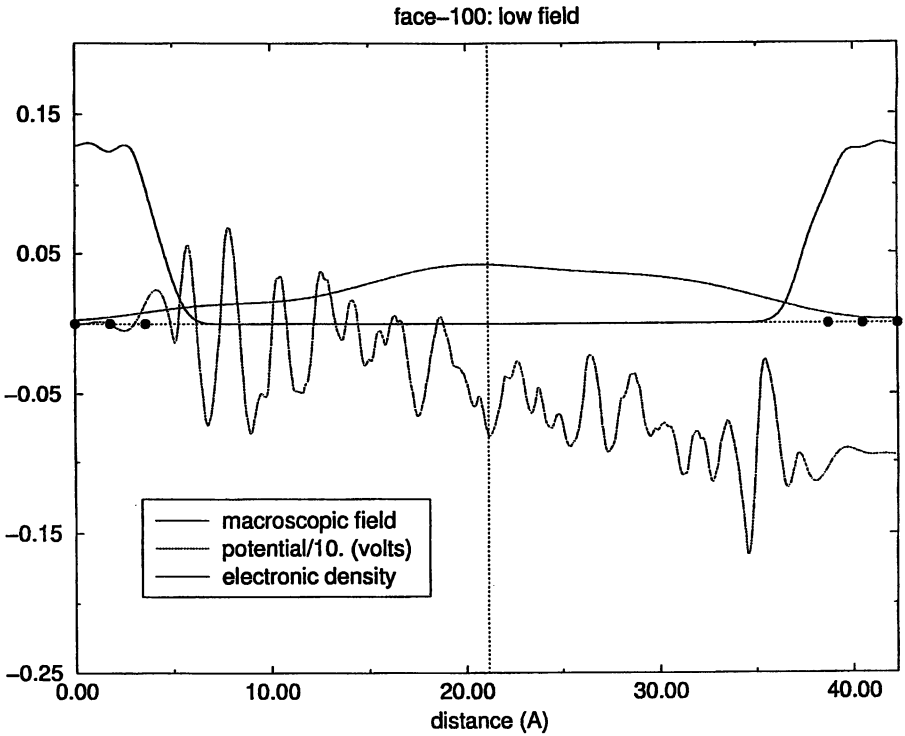

Figure 1. Electrostatic potential and clculated macroscopic electric fields are shown as a function of z for a fixed value of the charge σ on the electrodes. For reference purposes, the electron density is plotted along with solid circles indicating the position of copper centers. Units of the quantities shown are chosen for presentation purposes as E in V/Å, ϕ in V divided by 10 and electon density in e/au³ multiplied by 10. The 100 face is shown at charge σ= 10.3. Reprinted by permission from reference 1.

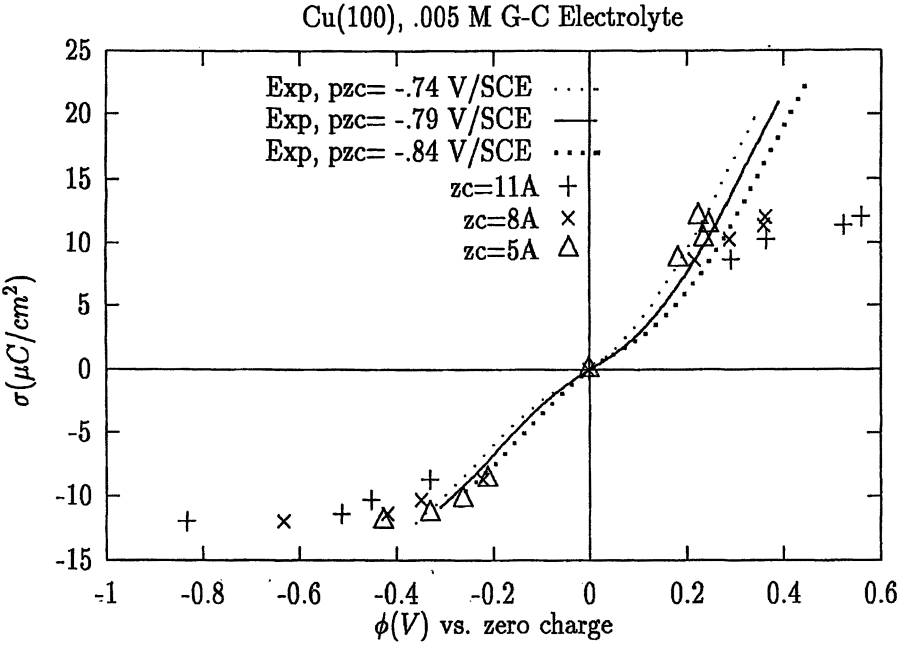

Figure 2. Calculated charge versus total potential drop for a 0.005 molar 1–1 electrolyte and various values of the matching distance z_c for the 100 surface. Integrated experimental results are shown from reference 17 with the zero of potential for the experimental results indicated. The reported potential of zero charge of reference 17 is −0.79 V/SCE for this surface. Reprinted by permission from reference 1.

surface, and in Figures 3 and 4 we compare experimental data from references 18 and 19 for the 111 surface. In each case we have shown the experimental results integrated to give $\sigma(\phi)$ and have chosen the zero of potential as the reported potential of zero charge of reference 18, namely –0.45 V/SCE and –0.79 V/SCE for the 111 and 100 surfaces, respectively. In addition we show the experimental curves assuming a potential of zero charge displaced by ±0.05V from the above values. For each surface the magnitude of the calculated capacitance is roughly consistent with the reported numbers of reference 18. For the 111 face, our capacitance values are larger than the results of reference 19 for all values of z_c. With regard to potential of zero charge for the copper–water interface, our results are not in disagreement with those of reference 17 . The experimental results are subject to significant uncertainties due to the reactivity of the copper electrode (*18– 21*), including surface oxidation, of which we take no account in the model.

The model of the electrostatic response of a copper electrode presented here exhibits features which are unique to our direct dynamics approach including the electronic structure of the electrode. The electron density at the surface displays an asymmetric response to electrode charging, as predicted qualitatively by more primitive models, but is here coupled correctly to the dynamics of the solvent and the Gouy–Chapman ionic screening. The macroscopic electric fields near the electrode–solvent interface are much more strongly screened than they are in models in which the electrode is treated classically.

Attempts at copper with d electrons

We examined the possibility of using direct dynamics simulation techniques like those used in the studies described above for explicit calculation of the equilibrium energetics and barrier heights in cuprous–cupric electron transfer, as we have done with classical models (*12*), by inclusion of a dissolved copper ion in the simulation. Earlier work done with the direct dynamics code has focused on bare electrodes in water, using purely local, semi–empirical pseudopotentials with which only the structure of the 4s electrons of the copper were calculated. Describing electron transfer with ionized copper centers requires a much larger calculation than these earlier efforts. Because the electronic structure of neutral copper is $[Ar]3d^{10}\,4s^1$, it is clear that a description of the oxidation process demands a simulation in which the 3d electrons are described explicitly. Tracking the dynamics of these more tightly bound electrons implies an increase in the number of wavefunctions calculated in the simulation as well as a substantial increase in the plane–wave cutoff energy (equivalently, a finer real–space mesh).

Table 1. Computational Cost of the Algorithm

Routine	*Scaling*	*Share (%, approximate)*
Orthogonalization	$M_\psi^2 N_G$	45
$H\psi$	$M_\psi N_G$	30
FFT	$M_\psi N_G \log N_G$	20

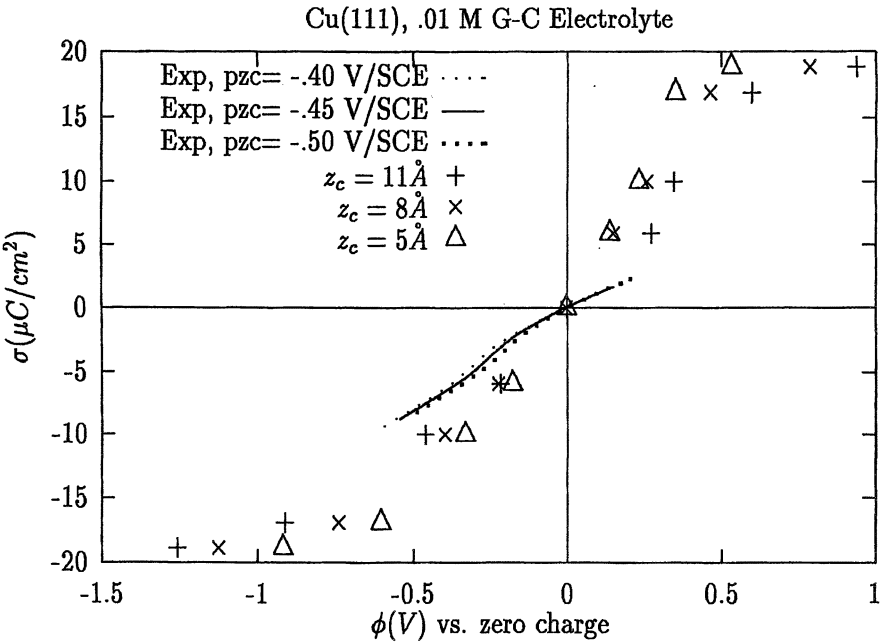

Figure 3. Same as Figure 2 , but for the 111 surface of copper. The reported potential of zero charge of reference 17 is −0.45 V/SCE for this surface. Reprinted by permission from reference 1.

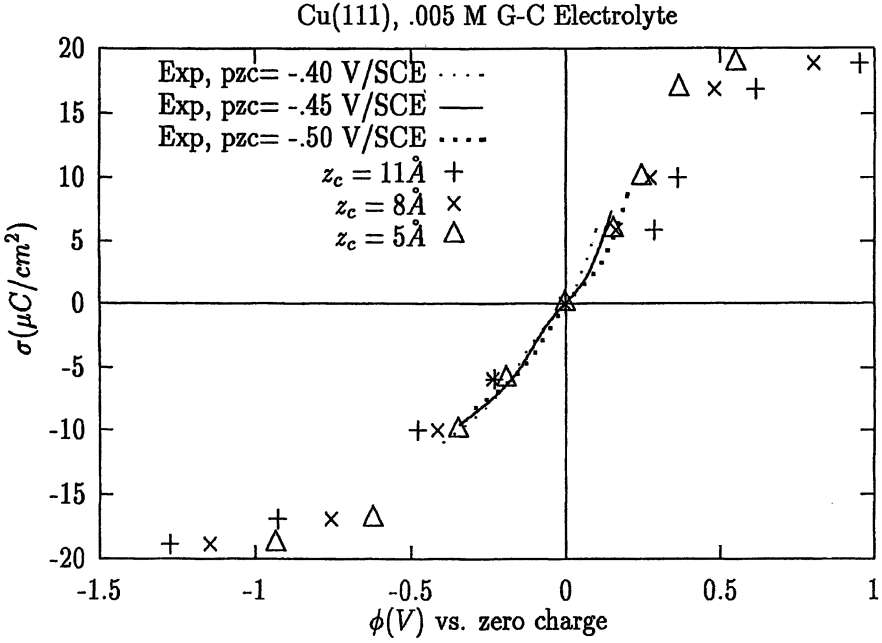

Figure 4. Same as Figure 3, but compared with the data of reference 18 , both theory and experiment with electrolyte concentration 0.01 M.Reprinted by permission from reference 1.

In the direct dynamics program, the computational cost of running the code on a typical system is dominated by three routines, as shown in table 1; the share of these routines of the total cost will vary depending on the values of M_ψ, the number of wavefunctions, and N_G, the number of plane–waves/grid points. The fourier transform ("FFT") is used in evaluating Hψ as $H\psi = T_G\psi_G + F^{-1}(V_R F\psi_G)$, where subscripts G and R refer to reciprocal and real space, respectively, T and V are the kinetic and potential energy operators, and F is the fourier transform operator.

To evaluate the LDA code for possible use in the electron transfer study, we carried out a number of preliminary calculations. The first was a calculation of the eigenvalues of a single, neutral 3d4s–copper atom (in vacuum with periodic boundary conditions). In agreement with the work from which the pseudopotential was derived(22), we found that a cutoff energy of about 80 Ry was necessary to converge the eigenvalues to satisfactorily match those of the all–electron calculation which generated the pseudopotential. This is a quite substantial increase over previous calculations, which were limited to 5 – 15 Ry. Calculations of an ionized atom yield energy differences which are in good agreement (error less than 3 percent) with experimental ionization energies, though absolute error values are significant on the electrochemical scale of tenths of volts.

To perform simulations of the electrode/electrolye interface, a simulation cell with a side length of 10 to 20 Å is required in order to minimize effects of the sample boundary on the system (in particular, the liquid component). For a copper electrode, this implies a slab with 5 to 6 atoms on a side, for a total of roughly 150 copper centers in the sample. The computational consequences of explicitly calculating the electronic structure of the 3d electrons on every copper atom are extreme; assuming the computation time scales with the orthogonalization step, which as described above is the most expensive part of the calculation, the increase in computation time for a fully described copper slab is on the order of 1000, which is prohibitively expensive at this time. To reduce this cost to the level of feasibility, several modifications were considered, including modification of the bases used to expand the wavefunctions, treating the electrode as a mixture of the 4s–copper in the bulk and the 3d4s–copper in regions where greater precision is necessary, and new methods of obtaining the ground state electronic density.

Initially, we considered using a more localized basis set than the traditional plane wave basis, inspired by the thought that the 3d electrons in the electrode are more tightly bound than the 4s. While transforming a quantity to any other complete basis would give a result with the same number of components N_G (i.e., no information is lost and hence the transforms are invertible), the advantage we sought in a different basis was that key quantities, such as the hamiltonian matrix or the wavefunctions, might be rendered sparse in a systematically exploitable way. Members of our group had previously explored the use of a Wannier basis which rendered the hamiltonian matrix in a sparse form; however, exploiting this sparseness in the calculation of H

was problematic, and the benefit of replacing the diagonal T_G and (semi) local V_R with a sparse $(T + V)_W$ in Wannier space was not clear.

A second option which we explored placed emphasis on reducing the cost of the expensive orthogonalization step. we introduced a systematic method of "basis thinning" or "zero suppression" in which, prior to orthogonalization, each wavefunction is scanned for components which are above a set threshold; an index vector of length $N_{thin} < N_G$ is stored which points only to these significant components, at a cost which scales as $M_\psi N_G$. In the orthogonalization loops, this results in the execution of

$$\psi'_2 = \psi_2 - \langle \psi_1 | \psi_2 \rangle \psi_1$$

in N_{thin} operations, rather than N_G. Thus with an overhead cost of order $M_\psi N_G$, the entire orthogonalization loop is reduced to order $M_\psi^2 N_{thin}$. We implemented this algorithm and found that the orthogonalization time is indeed reduced by applying the thinning mechanism, but the speedup at which the errors in quantities of interest become electrochemically intolerable is only about a factor of two. While this is a significant savings, it is not enough to make a full 3d4s–copper slab calculation affordable.

Next, we considered treating the bulk of the electrode slab as 4s–copper, with a "patch" of 3d4s–copper on the surface near where an additional 3d4s–copper ion would undergo the electron transfer reaction. Such a modification would greatly reduce the number of wavefunctions needed in the calculation, though the large cutoff energy would need to be retained in order to describe the few 3d4s–coppers accurately. This higher cutoff energy, however, could be exploited to use a truly first–principles pseudopotential for the 4s–copper (rather than the semi–emprically adjusted pseudopotential used in our group's previous studies). The cost, estimated at a factor of 20 more expensive than the earlier 4s–copper calculations, is on the edge of affordability. While a similar approach has been taken in small–cluster calculations of water adsorbtion on copper (*24*) , many theoretical issues need to be addressed in order for this to succeed. Included among these are evaluating the work function of the first–principles 4s–copper slab, assessing the impact of the patch on the work function, and estimating the quality of the interaction of the reacting ion with the patch, relative to the true interaction with a fully–described electrode.

As an initial test, we calculated the vacuum work function (defined in simulation as the difference between the electric potential in the vacuum region and the fermi level of the slab) of a 5x5x5 4s–copper slab exposing the (100) face, using ab initio pseudopotentials (*22*) at the cutoff energy required for 3d4s–copper convergence. The result at 5.8 eV disagrees with experimental results (*25*) of 4.5 eV by a large amount, indicating that, as feared, the 3d electrons play a significant role at the vacuum interface.

Rather than retrace the path of adjusting the pseudopotential to fit the work function as in reference 10, we considered more radical options to speeding up the calculation. A method which we developed based on the work of Goedecker and Teter (*26*) (with tight–binding electronic structure calculations) yields the ground state energy and electron density by applying the identity

$$\rho(x) = \sum_{\lambda} f(\epsilon_\lambda)\langle x|\lambda\rangle\langle\lambda|x\rangle$$
$$= \sum_{\lambda}\langle x|f(\beta(H-\mu))|\lambda\rangle\langle\lambda|x\rangle$$

with energy eigenstates $\{|\psi\rangle\}$, position eigenstates $\{|x\rangle\}$, and

$$f(x) = \frac{1}{e^x+1} = \sum_{n}^{M_H} a_n x^n$$

is the fermi function evaluated as a matrix polynomial. (In practice this is evaluated using Chebyshev polynomials.) In a model with purely local pseudopotentials, the density at all positions x can therefore be evaluated as

$$\rho(x) = \langle x|f(\beta(H-\mu))|\lambda\rangle$$

in $M_H N_G^2 \log N_G$ operations. Equivalently we can write in our plane–wave basis $\{|k\rangle\}$

$$\rho(x) = \sum_{k}\langle x|f|k\rangle\langle k|x\rangle$$

and introduce a vector of random phases

$$P = \sum_{k} e^{i\phi_k k}|k\rangle$$

to obtain

$$\langle x|f|P\rangle\langle P|x\rangle =$$
$$\sum_{k}\langle x|f|k\rangle\langle k|x\rangle + \sum_{k\neq k'} e^{i(\phi_k-\phi_{k'})}\langle x|f|k'\rangle\langle k|x\rangle$$
$$= \rho(x) + \delta\rho(x)$$

Hence summing over a sufficient number M_P of random vectors should give cancellation in $\delta\rho$ due to the randomness of the phases; indeed, self–averaging keeps $\delta\rho$ relatively small in a single vector. The energy can be evaluated as $E = V(\rho(x)) + 1/M_P \sum_P \langle P|T|P\rangle$.

Advantages of the method include the scaling of the number of operations in the case of local pseudopotentials as $M_H M_P N_G \log N_G$ which in particular is independent of the number of wavefunctions M_ψ and nearly order N_G. The method is easily parallelized (each processor generating a small number of approximate densities), and has low memory requirements. However, trials of the method required values on the order of $M_H \sim 10^3$ and $M_P \sim 10^2$ with $N_G \sim 10^5$, which if parallelized using $M_{cpu} \sim 10^2$ processors gives an estimated time of $10^{3+2+5-2}=10^8$, compared with the current algorithm at $M_\psi^2 N_G$ (orthogonalization step) which is $10^{2x2+5} = 10^9$; hence, this method also does not yield the required speedup. Evaluation of non–local pseudopotentials will significantly slow the hamiltonian multiplications in the evaluation of the fermi function. In addition, the process must be repeated with a number of chemical potentials to run with fixed electron number, further reducing its utility.

Hence, the daunting task of describing the large number of electronic wavefunctions at the spatial resolution required for accurate structural and energetic calculations poses
a severe challenge to current implementations of density functional theory. While our attempts to utilize the direct dynamics methods in the study of cuprous–cupric electron transfer have not yet met with success, we continue to explore many options and refine current methods.

Aluminum

While we are unable at this time to obtain a more complete description of the copper/water interface, it is a natural next step to consider one of the simpler sp metals. While our collaborator, David Price, has treated the cadmium/water interace, we have chosen for further study aluminum, which has 3 valence electrons per atom (electronic configuration $3s^2\ 3p^1$), due to its widespread use in industrial applications. We are also particularly interested in describing the complete series of interfaces in the aluminum metal / aluminum oxide / water system which is predominant in real–world applications. Though the electronically disorded structure of the oxide is not well suited for description by the direct dynamics code used here, studies of the metal/vacuum and metal/water interface are useful for our development of tight–binding methods for use in treating the oxide–containing interfaces (*27*).

We considered first a simulation cell containing 125 aluminum centers arranged in a 5x5x5 atom slab of FCC crystal structure exposing the 100 face to vacuum. Cell dimensions of 27.08 x 27.08 x 45.00 au were chosen to match the bulk lattice constant of aluminum metal. The aluminum centers were described with Troullier–Martins pseudopotentials (*22*) with a cutoff energy of 16 Ry for the plane–wave basis. Relaxation of the electronic density yielded a work function, defined as the difference between the electrostatic potential in the center of the vacuum region and

the fermi energy of the slab, of 4.49 eV, which compares well with the experimental value of 4.41 eV (*28*). The binding energy, defined as $E_{slab}/N - E_{atom}$ (and hence including surface energy contributions), is 3.65 eV (3.42 eV experimental (*28*)).

We next proceeded to allow the atomic centers of the aluminum slab to relax. Relaxation attempts with the copper slab, in which a semi–empirical pseudopotential was used, displayed large relaxations corresponding with the unsatisfactory energetics and geometry of small clusters of those pseudoatoms, which we have attributed to the neglect of the 3d copper electrons. We found, in contrast, that the Al_2 dimer using the Troullier–Martins pseudopotentials exhibited a binding energy in quite reasonable agreement with experiment (1.77 eV vs. 1.79 eV experimental (*30*)), but with a separation of 2.63 Å, somewhat larger than the expected 2.47 Å (*30*); hence, we expect the aluminum slab to expand to some extent. Since this was the first attempt at relaxation of the atomic centers using non–empirical pseudopotentials, we used the same supercell dimensions as in the case of the unrelaxed slab. In this case the expansion is constrained to the z direction, and hence its effects are exaggerated (Further studies varying the x– and y–dimensions of the simulation cell to allow symmetric relaxation of the slab are currently underway; we expect the geometric and energetic results to be bounded by those of the unrelaxed slab and the slab relaxed within the fixed supercell).

The slab was relaxed until the average force on the atomic centers was less than 0.01 eV/Å, with the maximum force less than 0.02 eV/Å. The relaxed slab exhibited a binding energy as defined above of 3.71 eV, with the outermost atomic layer displaced 0.18Å in the z direction from the position with bulk lattice structure, consistent with the error in the dimer geometry. The work function was reduced to 4.08 eV.

We have also begun a study of the aluminum slab in water using the water model described in reference 10. We introduced 180 water molecules into the simulation cell in an ice structure and have allowed them to thermally equilbrate to 300K with the electronic structure of the aluminum slab frozen. We have proceeded to allow the electronic structure to follow the motion of the water and look forward to allowing dynamics of the aluminum centers themselves.

Conclusions

We have studied the electrode/electrolyte interface using direct dynamics simulations. Inclusion of the electronic structure of the electrode has revealed qualitative differences in comparison with classical molecular dynamics simulations, in particular with regard to the capacitance of the interface and the character of electric fields near the electrode surface. Our studies of the copper/water interface have shown that, while it is possible to successfully treat the

electronic structure, the expense of such calculations currently prohibits the complete study of transition metals and their oxides, due to the large required number of wavefunctions and the high plane–wave cutoff energy necessary to resolve the wavefunctions. We have examined a number of alternative approaches to the electronic structure aspects in order to minimize this expense, but with limited success. However, we have been able to extend our studies to sp metals such as Aluminum, which, with the implementation of first–principles pseudopotentials, are allowing us to explore the effects of electrode nuclear relaxation and, in the near future, dynamics.

Acknowlegements

This work was supported in part by the National Science Foundatio, grant number DMR–952228, by the Department of Energy Office of Science, Materials Science Division grant number DE–FG02–91–ER45455 and by the University of Minnesota Supercomputing Institute.

Literature Cited

1. Walbran, S.; Mazzolo, A.; Halley, J. W.; Price, D. L.,J. Chem. Phys. 109, 8076 (1998)
2. Price, D.; Halley, J. W. *J. Electroanal. Chem.* **1983**, *150*, 347.
3. Halley, J.W.; Johnson, B.; Price, D.; Schwalm, M. *Phys. Rev. B* **1985**, *31*, 7695.
4. Halley, J. W.; Price, D. *Phys. Rev. B* **1987**, *35*, 9095.
5. Price, D.; Halley, J. W. *Phys. Rev B* **1988**, *38*, 9357.
6. Schmickler, W.; Henderson, D. *J. Chem. Phys.* **1986**, *85*, 1650.
7. Goodisman, J. *J. Chem. Phys.* **1989**, *90*, 5756.
Amokrane, S.; Russier, V.; Badiali, J.P. *Surf. Sci.* **1989**, *217*, 425.
8. Kornyshev, A.A. *Electrochim. Acta* **1989**, *34*, 1829.
9. Price, D.; Halley, J. W. *J. Chem. Phys.* **1995**, *102*, 6603.
10. Bard, A. J.; Faulkner, L. R. Electrochemical Methods, Fundamentals and Applications, J. Wiley and Sons: NY, 1980; p. 500
11. Halley, J.W.; Walbran, S.; Smith, B. Proceedings of the Workshop on Charge Transfer at ITCP Trieste, ed. Kornyshev, A.; World Scientific, 1997.
12. Stern, O. *Z. Elektrochem.* **1924**, *30*, 508.
13. Toukan, K.; Rahman, A. *Phys. Rev. B* **1985**, *31*, 2643.
14. Hautman, J.; Halley, J. W.; Rhee, Y.–J. *J. Chem. Phys.* **1989**, *91*, 467.
15. Halley, J. W.; Walbran, S.; Price, D. L. Interfacial Electrochemistry, ed. Wieckowski, A. Marcel Dekker: New York, in press.
16. Jackson, J. D. Classical Electrodynamics; J. Wiley and Sons: New York, 1975; Sec. 6.7.

17. Lecoeur, J.; Bellier, J. P. *Electrochimica Acta* **1985,** *30*, 1027.
18. Haertinger, S.; Doblhofer, K. *J. Electroanal. Chem.* **1995,** *380* , 185.
19. LaGraff, J.R.; Cruickshank, B.J.; Gewirth, A.A. *In .. Nanoscale Physical Properties of Materials..MRS Symp.*; Sarikaya, M.; Wickramasinghe, H.K.; Isaacson, M., Eds. MRS: Pittsburgh, PA, 1994; p.121.
20. Foresti, M. L.; Pezzatini, G.; Innocenti, M.. *J. Electroanal. Chem.* **1997,** *434*, 191.
21. Troullier, N.; Martins, J. L. *Phys. Rev. B* **1991**, *43*, 1993.
22. Walbran, S. *Doctoral Thesis*, University of Minnesota; 1999.
23. Ribarsky, M. W.; Luedtke, W. D.; Landman, U. *Phys. Rev. B* **1985**, *32*, 1430.
24. Lipkowski, J.; Ross, P.N. *Structure of Electrified Interfaces*; VCH Publishers: New York, NY, 1993; p 213.
25. Goedecker, S.;Teter, M. *Phys. Rev. B* **1995**, *51*, 9455.
26. Schelling, P.K. , Halley, J. W., Yu, N. *Phys. Rev. B* **1998,** *51,*1279
27. Lide, D. R., ed., *Handbook of Chemistry and Physics*, 77th ed. Chemical Rubber Cleveland, 1997, p10–214
28. Cox, J. D.; Wagman, D. D.; Medvedev, V. A. *CODATA Key Values for Thermodynamics*; Hemisphere Publishing Corp.: New York, 1989.
29. Huber, K. P.; Herzberg, G. *In NIST Chemistry WebBook, NIST Std. Ref. Database 69*; Mallard, W.G.; Linstrom, P.J., Eds. NIST: Gaithersburg, MD, 2000; (http://webbook.nist.gov)